Environmental Science
Water Research & Technology

# Glycerol-driven Denitratation: Process Kinetics, Microbial Ecology, and Operational Controls



| | |
|---|---|
| Journal: | *Environmental Science: Water Research & Technology* |
| Manuscript ID | EW-ART-09-2021-000700.R1 |
| Article Type: | Paper |
| | |

## Water Impact Statement

This study's characterization of denitratation could, in conjunction with downstream anammox, yield a more sustainable alternative to chemical- and energy-intensive conventional nitrification and denitrification. The findings have an immediate and long-term influence on WRRFs incorporating short-cut BNR processes driven by glycerol. Results were subsequently used to propose bioreactor operating strategies that could maximize nitrite accumulation in real-world denitratation systems.

# Glycerol-driven Denitratation: Process Kinetics, Microbial Ecology, and Operational Controls

AUTHOR NAMES: *Matthew P. Baideme,*[a,#] *Chenghua Long,*[a] *Luke T. Plante,*[a,b] *Jeffrey A. Starke,*[b,1] *Michael A. Butkus,*[b] *and Kartik Chandran*[a,*]

AUTHOR AFFILIATIONS:

[a] Department of Earth and Environmental Engineering, Columbia University, New York, NY 10027, U.S.A.

[b] Department of Geography and Environmental Engineering, United States Military Academy, West Point, NY 10996, U.S.A.

[1] Present address: Opus College of Engineering, Marquette University, Milwaukee, WI 53201, U.S.A.

[#] Co-corresponding author: Department of Earth and Environmental Engineering, Columbia University, 500 W. 120th St., New York, NY 10027. Email: mpb2177@columbia.edu.

[*] Co-corresponding author: Department of Earth and Environmental Engineering, Columbia University, 500 W. 120th St., New York, NY 10027. Email: kc2288@columbia.edu. Phone: 212.854.9027. Fax: 212.854.7081.

ABSTRACT: Denitratation, the selective reduction of nitrate to nitrite, is a novel process when coupled with anaerobic ammonium oxidation (anammox) could achieve resource-efficient biological nitrogen removal of ammonium- and nitrate-laden waste streams. Using a

fundamentally-based, first principles approach, this study optimized a stoichiometrically-limited, glycerol-driven denitratation process and characterized mechanisms supporting nitrite accumulation with results that aligned with expectations. At the optimal influent chemical oxygen demand to nitrate ratio of 3.0:1 identified, glycerol supported selective nitrate reduction to nitrite (nitrite accumulation ratio, NAR=62%) and near-complete nitrate conversion (nitrate reduction ratio, NRR=96%), indicating its viability in a denitratation system. Specific rates of nitrate reduction (135.3 mg-N/g-VSS/h) were at least one order of magnitude greater than specific rates of nitrite reduction (14.9 mg-N/g-VSS/h), potentially resulting in transient nitrite accumulation and indicating glycerol's superiority over other organic carbon sources in denitratation systems. Optimal stoichiometric limitation pH and ORP inflection points in nitrogen transformation assays corresponded to maximum nitrite accumulation, indicating operational setpoints to prevent further nitrite reduction. Denitratation conditions supported enrichment of *Thauera* sp. as the dominant genus. Stoichiometric limitation of influent organic carbon, coupled with differential nitrate and nitrite reduction kinetics, optimized operational controls, and a distinctively enriched microbial ecology, was identified as causal in glycerol-driven denitratation.

KEYWORDS: partial denitrification; denitratation; glycerol; short-cut biological nitrogen removal; first-principles approach

## 1. Introduction

Conventional biological nitrogen removal (BNR), including energy and chemical-intensive nitrification and denitrification, is traditionally used to treat ammonium-laden ($NH_4^+$)

waste streams. The advent of engineered processes that achieve oxidation of $NH_4^+$ to nitrite ($NO_2^-$), termed nitritation, combined with denitritation (reduction of $NO_2^-$ to nitrogen gas ($N_2$)) or anaerobic ammonium oxidation (anammox) represent short-cut BNR alternatives to conventional BNR approaches. Such short-cut BNR processes can provide reductions in chemical (external carbon for denitrification and alkalinity for nitrification) and energy use (aeration for nitrification), driving the desire for $NO_2^-$ accumulation within these processes.[1]

Alternatively, waste streams containing concomitantly high concentrations of $NH_4^+$ and nitrate ($NO_3^-$), such as those resulting from fertilizer[2] and explosives manufacturing,[3,4] provide similar energy and chemical reduction opportunities through distinct short-cut BNR processes. A particularly effective pathway for treating waste streams containing both $NH_4^+$ and $NO_3^-$ is through heterotrophic[5–10] or autotrophic[11] denitratation (selective reduction of $NO_3^-$ to $NO_2^-$) coupled with downstream anammox. A combined denitratation-anammox system used to treat waste streams containing equal concentrations of $NH_4^+$ and $NO_3^-$, such as those previously described, would theoretically reduce aeration energy requirements by 100% and COD requirements by 60% compared to treatment of the same waste stream using conventional BNR.[12] These benefits translate to municipal wastewater treatment as well, with a 50% decrease in aeration energy and 80% in COD requirements for a partial nitrification-denitratation-anammox system.[12] Recent studies[5–10] on heterotrophic denitratation have focused on performance in lab-scale sequencing batch reactors (SBRs) driven by acetate, methanol, glucose, and sludge fermentation liquid due to the lack of sufficient readily biodegradable chemical oxygen demand (COD) in typical waste streams. These studies have primarily been observational in nature, with particular emphasis placed on empirically identifying parameters and conditions that potentially contributed to $NO_2^-$ accumulation, such as influent COD:N ratios,

pH, ORP, and loading rates. Stoichiometric limitation of influent COD:N ratios, specifically, has been shown to influence endpoint nitrogen speciation.[13] Various parameter combinations were optimized, denoted by the observation of stable $NO_3^-$-to-$NO_2^-$ conversion ratios as high as 90% during steady-state studies.[7]

The selection of an external COD source to drive denitrification is critical when attempting to maximize $NO_2^-$ accumulation. Traditionally, methanol has been one of the most widely used external COD sources for denitrification due to its low cost and wide availability.[14] $NO_2^-$ accumulation has proven difficult with methanol due to methanol dehydrogenase's direct delivery of electrons to cytochrome *c* and proximal to $NO_2^-$ reductase as opposed to distribution solely through the ubiquinol pool to $NO_3^-$ reductase similar to other carbon sources.[15–17] The unique electron delivery locations during methanol oxidation within the respiratory denitrification chain potentially contribute to concomitant $NO_3^-$ and $NO_2^-$ reduction.

Several water resource recovery facilities are switching to glycerol due to the operational and safety risks associated with methanol.[14] Glycerol is similar in cost to methanol and less expensive than ethanol and acetate,[18–20] is available as a waste or byproduct,[21,22] and has no known inhibitory effects on the anammox process, unlike methanol.[23] $NO_2^-$ accumulation during glycerol supplementation was also anecdotally observed in full-scale treatment plants resulting in unintentional enrichment of anammox on the produced $NO_2^-$.[24] Nevertheless, to fully realize the operating benefits that a denitratation-anammox system could offer, it is imperative for the parameters and conditions leading to $NO_2^-$ accumulation in a glycerol-driven denitratation system to be systematically identified, defined, and addressed in relation to reactor operating strategies.

Accordingly, the overarching goals of this study were to use a fundamentally-based, first principles approach to characterize the process kinetics, nitrogen conversion efficiencies, and microbial ecology of a glycerol-fed denitratation process, and identify concomitant reactor operating strategies. The specific objectives were to (1) control selective conversion of $NO_3^-$ to $NO_2^-$ through stoichiometric limitation of influent glycerol dose, (2) quantify the rates of $NO_3^-$ reduction relative to rates of $NO_2^-$ reduction and understand their impact on the selective accumulation of $NO_2^-$, (3) elucidate the microbial community structure under varied carbon-loading levels in a functional glycerol-driven denitratation process, and (4) identify operational controls and reactor operating strategies to maximize denitratation rates and efficiencies.

## 2. Materials and Methods

### 2.1. Experimental Set-up and Reactor Operation

A lab-scale SBR with a working volume, V=12 L, was operated at room temperature (22±2°C) for a period of 232 d. The SBR was operated at a hydraulic retention time (HRT) of 1 d, utilizing 4 cycles per day with each cycle consisting of a 90-min anoxic feed and react period, a 180-min anoxic react period, a 50-min settling period, and a 40-min decant period. SBR feed contained 100.0 mg/L $NO_3^-$-N as the terminal electron acceptor to simulate the influent of a high $NO_3^-$-containing waste stream typical of a fertilizer[2] or explosives[3] manufacturing facility, 25.0 mg/L $NH_4^+$-N (to support assimilation), and macro and trace nutrients (Table S1). $NH_4^+$ availability supported cell growth with a more easily assimilable nitrogen source, maximizing metabolic energy generation via $NO_3^-$ reduction as opposed to assimilation. pH was controlled automatically at 7.50±0.05 using 0.5 M HCl and 1.0 M $NaHCO_3$ via a chemical dosing pump (Etatron D.S., Italy). Sludge wasting was controlled daily at the end of the anoxic feed and react

period following COD exhaustion to maintain a solids retention time (SRT) of 3 d. Glycerol, diluted to a 15% solution by volume, served as the external COD source and was provided to meet influent COD:$NO_3^-$-N ratios from 2.5:1 to 5.0:1. Glycerol was fed at the end of the anoxic feed and react period so that examined influent COD:$NO_3^-$-N ratios were met during each cycle. Upon transitioning to each influent COD:$NO_3^-$-N ratio tested, the SBR was determined to be at steady-state once all biomass concentrations were within ±10% over the course of one SRT period after which a stabilization period of 4 x SRT was allocated to allow for sludge acclimation prior to assessing performance relative to other conditions. Sequencing and timing of SBR cycles and daily solids wasting was controlled and maintained by peristaltic pumps (Masterflex, IL) using electronic timers (ChronTrol Corporation, CA).

## 2.2. Sample Collection and Wastewater Quality Analysis

All analytical procedures employed were in accordance with Standard Methods for the Examination of Water and Wastewater.[25] Aqueous-phase samples were withdrawn during the decant period of the reactor cycle and concurrently from the influent for chemical species analysis after centrifugation (8,000 x G, 10 min, 4-8ºC) to remove cells and cell debris. $NO_3^-$ and $NH_4^+$ were measured using ion selective electrodes (Thermo Fisher Scientific, MA). $NO_2^-$ concentration was measured via diazotization and colorimetry.[25] The fraction of influent $NO_3^-$ lost to nitrogenous gases was determined via mass balance on nitrogen. Centrifuged aqueous-phase samples were filtered using 0.20 µm syringe filters (A Chemtek, MA) and stored at -20ºC. Dionex ICS-2100 ion chromatography using a Dionex IonPac AS-18 IC column (Thermo Fisher Scientific, MA) was used to confirm ion selective electrode and colorimetric measurements of $NO_3^-$ and $NO_2^-$ concentrations, respectively. Similarly, a Dionex IonPac AS-14 IC column

(Thermo Fisher Scientific, MA) was used to quantify volatile fatty acid production during unbuffered *ex situ* batch kinetic assays. Separate aqueous-phase samples were extracted at the end of the anoxic react period and during the decant period of the reactor cycle to assess total biomass concentrations in the reactor and effluent, respectively, for SRT control. Aqueous-phase samples taken during the decant period were centrifuged (8,000 x G, 10 min, 4-8ºC) and filtered using 0.45 µm syringe filters (A Chemtek, MA) to assess remaining soluble COD (sCOD) concentrations (Hach Chemical Company, CO). Biomass concentrations were approximated by subtracting sCOD measurements from total COD measurements to determine particulate COD (pCOD) (Hach Chemical Company, CO).[26] Additional aqueous-phase samples taken just prior to the end of the anoxic react period were centrifuged (8,000 x G, 10 min, 4-8ºC), supernatant was discarded, and cell pellets were preserved at -80ºC for subsequent DNA extraction and 16S rRNA gene sequencing at all influent COD:$NO_3^-$-N ratios tested except for influent COD:$NO_3^-$-N=2.8:1.

## 2.3. Feeding Strategy Experiments

Two feeding strategies were evaluated to maximize $NO_2^-$ accumulation during experiments conducted following the 232 d operational period. A semi-continuous feeding strategy delivered $NO_3^-$-containing SBR feed and glycerol continuously for the first 75 and 72 min, respectively, of the anoxic feed and react period (Fig. S1). A pulse feeding strategy delivered a pulse of $NO_3^-$-containing SBR feed and glycerol every 45 min for the first 270 min of the SBR cycle (Fig. S1). Feeding rates were controlled to maintain equivalent mass loading rates of $NO_3^-$ and glycerol and influent COD:$NO_3^-$-N ratios for the two feeding strategies.

160 2.4. Batch kinetic assays

161 Batch assays, *in situ* (within the SBR) and *ex situ*, were conducted to measure extant
162 process kinetics and optimize operational controls, including batch duration, pH, and ORP. *In*
163 *situ* assays followed previously described sampling collection and chemical analysis procedures.
164 Aqueous-phase samples were obtained from the primary SBR at steady-state over the course of a
165 single 360-min reactor cycle. *Ex situ* assays were carried out in an anoxic, sealed, spinner flask
166 batch vessel with a working volume, V=1 L, at room temperature (22±2$^{o}$C). Mixed liquor was
167 taken from the primary SBR at steady-state during the feed and react period, washed 4 times
168 using SBR feed without $NO_3^-$, and supernatant was discarded. Prior to extant kinetic batch
169 assays, the medium was buffered to pH 7.50 using 0.5 M HCl and 1.0 M $NaHCO_3$ and $N_2$ gas
170 was sparged until dissolved oxygen (DO) levels were equal to 0.01 mg/L $O_2$, or the minimum
171 practical limit of the InPro 6850i polarographic DO sensor with M300 transmitter (Mettler-
172 Toledo, OH). pH was maintained at pH 7.50±0.05 by manual control.

173 pH optimization batch assays were conducted within normal pH operating ranges (see
174 Supporting Information (SI)). $NO_3^-$ and glycerol were dosed to meet the desired initial
175 COD:$NO_3^-$-N ratio. $NO_3^-$ was dosed at the outset of the experiment (time=0 min) and the
176 biomass was incubated for 30 min prior to the addition of glycerol to ensure that residual
177 nitrogen species and glycerol from the primary SBR remaining in the washed mixed liquor were
178 consumed prior to data collection. pH, ORP, and DO were measured and recorded continuously
179 via an InPro 3253i/SG pH/ORP electrode and an InPro 6850i polarographic DO sensor,
180 respectively, attached to an M300 transmitter (Mettler-Toledo, OH).

181 Following extant kinetic batch assays, linear regression with $R^2 \geq 95\%$ of $NO_x$-N species
182 from time points of maximum concentration to minimum concentration for each respective

species was performed with pCOD concentrations taken just prior to glycerol input to determine true specific rates of $NO_3^-$ reduction (sDNaR) (Eqn. 1) and $NO_2^-$ reduction (sDNiR) (Eqn. 2). $NO_2^-$ production resulting from $NO_3^-$ reduction was not accounted for in the determination of specific rates of $NO_2^-$ reduction, yet this remains representative of a true reduction rate. During the time points assessed for each influent COD:$NO_3^-$-N ratio, $NO_3^-$ removal was complete or near-complete (<3% of initial dose) except at influent COD:$NO_3^-$-N=2.5:1 where $NO_3^-$ concentration measurements confirmed no continued $NO_3^-$ reduction. pCOD measurements were used to determine maximum specific substrate consumption rates (Eqns. 1-2).

$$sDNaR = \left(\frac{1}{X}\right)\left(\frac{\Delta S_{NO_3^-}}{\Delta t}\right) \quad \textbf{Eqn. 1}$$

$$sDNiR = \left(\frac{1}{X}\right)\left(\frac{\Delta S_{NO_2^-}}{\Delta t}\right) \quad \textbf{Eqn. 2}$$

Where:

*sDNaR*: maximum specific $NO_3^-$ consumption rate (mg $NO_3^-$-N/g VSS/h)

*sDNiR*: maximum specific $NO_2^-$ consumption rate (mg $NO_2^-$-N/g VSS/h)

*X*: volumetric biomass concentration approximated using pCOD measurements (g VSS/L)

$\frac{\Delta S_{NO_3^-}}{\Delta t}$: volumetric substrate ($NO_3^-$) consumption rate (mg $NO_3^-$-N/L/h)

$\frac{\Delta S_{NO_2^-}}{\Delta t}$: volumetric substrate ($NO_2^-$) consumption rate (mg $NO_3^-$-N/L/h)

2.5. DNA Extraction, Next-Generation Sequencing of Amplicon Library, and Bioinformatics

DNA was extracted from biomass samples and purified using a QIAamp DNA Mini Kit (Qiagen, Inc., MD). The quality and quantity of DNA were checked using a NanoDrop Lite spectrophotometer (Thermo Fisher Scientific, MA). Barcoded fusion primers with Ion Xpress™ sequencing adapters (Thermo Fisher Scientific, MA) and a 16S rRNA bacterial 1055F/1392R universal primer set were applied in each sample for multiplex sequencing. Amplification of genomic DNA targets was performed with iQ™ SYBR® Green Supermix (Bio-Rad, CA) and purification via Agencourt AMPure XP Reagent (Beckman Coulter, CA). Library quantification was performed with an Agilent DNA 1000 Kit (Agilent, CA). Template preparation with the DNA library followed by Ion Spheres Particle (ISP) enrichment was performed using Ion OneTouch2 (Ion PGM Hi-Q View OT2 Kit). Enriched ISP was loaded onto an Ion Torrent 318 v2 BC chip and run on an Ion Torrent Personal Genome Machine (Ion PGM Hi-Q View Sequencing Kit). Ion Torrent Suite software was used for base calling, signal processing, and quality filtering (Phred score of >15) of the raw sequences. The 1055F/1392R universal primer set targeted sequences of approximately 350 base pairs (bp). Mothur software was used to initially screen out likely incorrect amplicon sequences with bp lengths more than 50 bp different than the target sequence length.[27] AfterQC software was utilized to further delete bad quality reads (Phred score of <20) and trim the tails of reads where quality dropped significantly.[28] DADA2 programming via R Studio software was used to produce a table of non-chimeric amplicon sequence variants from the demultiplexed fastq files.[29] QIIME2 software was applied in conjunction with the Silva version 132 reference taxonomy for further post-sequencing bioinformatic analysis.[30] Principal Coordinates Analysis (PCoA) plot was generated through R Studio ggplot2 package.

227

228 2.6. Nitrogen Conversion Calculations

229 Reactor performance was normalized with respect to the influent characteristics. A $NO_2^-$
230 accumulation ratio (NAR) (Eqn. 3) was defined to relate the accumulation of $NO_2^-$ to the
231 removal of $NO_3^-$.[31] A NAR equal to 100% indicated that all $NO_3^-$ removed accumulated as $NO_2^-$
232 compared to terminal reduction to $N_2$ gas, for which the NAR would be 0%. $NO_3^-$ reduction was
233 also classified in terms of a $NO_3^-$ reduction ratio (NRR) (Eqn. 4), which normalized the
234 conversion of $NO_3^-$ to the influent $NO_3^-$ concentration.[10] A NRR equal to 100% would indicate
235 conversion of all influent $NO_3^-$ to any reduced form, while a NRR of 0% would indicate no
236 conversion.

237

238 $$NAR = \left[\frac{(NO_{2,eff}^- - N) - (NO_{2,inf}^- - N)}{(NO_{3,inf}^- - N) - (NO_{3,eff}^- - N)}\right] x\ 100\% \quad \textbf{Eqn. 3}$$

239

240 $$NRR = \left[\frac{(NO_{3,inf}^- - N) - (NO_{3,eff}^- - N)}{(NO_{3,inf}^- - N)}\right] x\ 100\% \quad \textbf{Eqn. 4}$$

241

242 Where:

243 $NO_{2,inf}^- - N$: influent $NO_2^-$-N concentration (mg $NO_2^-$-N/L)

244 $NO_{2,eff}^- - N$: effluent $NO_2^-$-N concentration (mg $NO_2^-$-N/L)

245 $NO_{3,inf}^- - N$: influent $NO_3^-$-N concentration (mg $NO_3^-$-N/L)

246 $NO_{3,eff}^- - N$: effluent $NO_3^-$-N concentration (mg $NO_3^-$-N/L)

247

248 3. Results and Discussion

249 3.1. Denitratation Reactor Performance

250 The influent COD:$NO_3^-$-N ratio required for glycerol-driven denitrification ($NO_3^-$-N to $N_2$
251 reduction) was thermodynamically[32] determined to be 5.9:1 (see SI). This corresponded well
252 with experimentally-determined operational ratios of 5.0:1 to 5.6:1. Stoichiometric analysis
253 revealed that influent COD:$NO_3^-$-N=2.4:1 (see SI) would provide only enough electrons via
254 COD oxidation to reduce $NO_3^-$ to $NO_2^-$ on a theoretical electron equivalence basis as opposed to
255 full denitrification. Therefore, influent COD:$NO_3^-$-N ratios between 2.4:1 and 5.9:1 were
256 referred to as stoichiometrically-limited for the purposes of this study. These calculations form
257 the fundamentally-based foundation to the first principles approach used in this study to conduct
258 and interpret the results of glycerol-driven denitratation presented herein.

259 The utilization of glycerol as the external COD source and electron donor resulted in
260 significant $NO_2^-$ accumulation at stoichiometrically-limited influent COD:$NO_3^-$-N ratios from
261 2.5:1 to 5.0:1, indicating that the use of glycerol was feasible to sustain a denitratation process.
262 The highest degrees of $NO_3^-$ removal and $NO_2^-$ accumulation, as a function of influent
263 COD:$NO_3^-$-N ratio during steady-state SBR operation, occurred at influent COD:$NO_3^-$-N=3.0:1
264 (Fig. 1). This resulted in an average $NO_2^-$ accumulation of 60.8±11.5 mg/L $NO_2^-$-N (n=10) and
265 NAR of 62%, indicating that 62% of the $NO_3^-$ reduced was converted to $NO_2^-$ rather than
266 terminally reduced to $N_2$ gas. Additionally, the NRR was determined to be 96%, indicating that
267 a majority of the influent $NO_3^-$ was converted leaving only approximately 4% of influent $NO_3^-$ in
268 the effluent (Table 1). Accumulation of $NO_2^-$ at influent COD:$NO_3^-$-N=3.0:1 compared to
269 influent COD:$NO_3^-$-N=4.0:1 ($p=0.21$, $\alpha=0.05$, $n=7$) and influent COD:$NO_3^-$-N=2.8:1 ($p=0.49$,
270 $\alpha=0.05$, $n=10$) was not significantly different. Similar NAR and NRR at influent COD:$NO_3^-$-

N=3.0:1 and 4.0:1 indicated that influent COD:$NO_3^-$-N=3.0:1 was more operationally optimal due to the lesser required COD loading to achieve analogous performance. COD loading should be minimized in a single-stage denitratation-anammox or in a denitratation system feeding downstream anammox due to the negative impacts excess COD impart on anammox.[33]

Substantial $NO_3^-$ accumulation occurred at influent COD:$NO_3^-$-N=2.8:1 (31.7±11.4 mg/L $NO_3^-$-N, n=11), signifying that this ratio was less operationally optimal compared to influent COD:$NO_3^-$-N=3.0:1. The observed $NO_3^-$ accumulation at influent COD:$NO_3^-$-N=2.5:1 and 2.8:1 may be due to lower biomass concentrations (Table S2) requiring longer batch durations to accomplish additional $NO_3^-$ conversion through increased reaction time. However, effluent sCOD concentrations were negligible (<3.7%; Table S2) signifying that glycerol was nearly completely consumed within the examined batch duration. Rather, the observed $NO_3^-$ accumulation in these cases indicated that the influent COD:$NO_3^-$-N was not sufficient despite the stoichiometric compliance of these influent COD:$NO_3^-$-N ratios,[10] potentially due to unrealized COD requirements for cell maintenance and synthesis[34] or additional demand by non-denitrifying[35] or fully-denitrifying microorganisms remaining in the microbial community. Therefore, influent COD:$NO_3^-$-N=3.0:1 was deemed more optimal than influent COD:$NO_3^-$-N=2.8:1 due to the similar $NO_2^-$ accumulation coupled to less than 4% of the influent $NO_3^-$ remaining in the effluent. The high sensitivity at influent COD:$NO_3^-$-N<3.0:1 highlighted significant implication for accurate system operation and control. A minimal reduction in influent COD:$NO_3^-$-N ratio from 3.0:1 to 2.8:1 yielded a sevenfold increase in effluent $NO_3^-$, signifying that strict control of the glycerol-driven denitratation system must be maintained. To this end, online dosing control[19] based on appropriate signals of reactor performance seems

necessary to maximize concomitant $NO_3^-$-N conversion selectively to $NO_2^-$ during partial denitratation.

Analysis of variance (ANOVA) across the influent COD:$NO_3^-$-N ratios identified a statistically significant difference in NAR ($p=4.8x10^{-11}$, $\alpha=0.05$, n=38) with a decrease from 69% to 11% as the influent COD:$NO_3^-$-N ratio approached that for glycerol-driven denitrification (5.9:1; see SI). Further Holm-Sidak post-hoc multiple comparison analysis indicated that the significant difference in NAR was primarily caused by the expectedly lower NAR at influent COD:$NO_3^-$-N=5.0:1 ($p<9.7x10^{-5}$ for all comparisons, $\alpha=0.05$; Table S3). The decrease in NAR from influent COD:$NO_3^-$-N=4.0:1 to 5.0:1 was most likely attributable to excess available COD that was used to further reduce accumulated $NO_2^-$ to gaseous nitrogen products. No significant difference in NAR (Table S3) was identified between influent COD:$NO_3^-$-N ratios of 3.0:1 (NAR=62%) and 4.0:1 (NAR=57%), further supporting that similar $NO_2^-$ accumulation could be achieved at lower influent COD:$NO_3^-$-N ratios while maintaining near-complete $NO_3^-$ removal.

Previous studies[5,7] observed that varying the influent COD:$NO_3^-$-N ratio had a negligible effect on the NAR determined at the point of maximum $NO_2^-$ accumulation during *ex situ* batch experiments, while a separate batch study[36] concluded that the COD source, as opposed to the influent COD:$NO_3^-$-N ratio, impacted the NAR more readily. In contrast, another separate batch study[8] concluded that $NO_2^-$ accumulation was influenced by both the COD source and COD dosing. While insightful, the utility of these results[5,7,8] to guide steady-state denitratation processes is limited as these studies failed to acclimate their batch experiment seed sludge to the conditions being investigated, which likely contributed to their discrepancy with the current study. Despite investigating the impact of various influent COD:$NO_3^-$-N ratios, Ge et al.[8] utilized a fully denitrifying inoculum, whereas Du et al.[7] inoculated batch experiments assessing

316 various influent COD:$NO_3^-$-N ratios with a microbial community acclimated to a single
317 stoichiometrically-limited influent COD:$NO_3^-$-N ratio. Both seed sludges likely contained
318 phenotypes with $NO_2^-$ accumulation capabilities different than those expected following
319 acclimation to the investigated conditions. Cao et al.[5] did not report conditions of their batch
320 inoculum.

321 In an improvement over these previous efforts, our current study utilized a sludge
322 stabilization and acclimation period of 4 x SRT following influent COD:$NO_3^-$-N ratio changes.
323 This intentionally allowed the microbial community to adapt to the influent COD:$NO_3^-$-N ratio
324 being investigated. In doing so, it was observed that the influent COD:$NO_3^-$-N ratio had similar
325 impacts on NAR during both steady-state operation (Fig. 1) and *ex situ* batch assays, with $NO_2^-$
326 accumulation decreasing as influent COD:$NO_3^-$-N ratios increased (Fig. S2).

327 In comparison to other steady-state operation studies[7,10,37] using primarily sodium acetate
328 as the external COD source, glycerol-driven NARs were at least 10% lower (Table 1). While
329 most reported acetate-driven denitratation NARs were greater than 80%, glycerol-driven
330 denitratation yielded NARs less than 70%. These respective acetate-driven steady-state
331 studies[7,10,37] were deemed reasonable comparisons due to similar COD dosing regimens and
332 results were reported for study periods sufficient in length to assume microbial community
333 acclimation to and stabilization at the studied conditions. Despite this, the assessment of reactor
334 performance based solely upon reported NARs can be misleading as the index does not account
335 for complete or other conversion of influent $NO_3^-$. Thus, NAR=100% does not necessarily
336 indicate that all influent $NO_3^-$ was converted. Several studies,[5–7,37] however, reported NRRs of
337 nearly 100% that when coupled with a NAR approaching 100% indicated near-perfect
338 denitratation performance (Table 1). It follows then that optimal performance in the current

study occurred at influent COD:$NO_3^-$-N=3.0:1 with NAR=62% and NRR=96%. The inability of glycerol to achieve similar efficiency to acetate- or fermentate-driven denitratation is not currently understood. Possible explanations include a greater intracellular carbon and microbial energy storage mechanism during low substrate availability,[38,39] the COD-source supported enrichment of a microbial consortium with a greater abundance of true denitrifiers,[35] an inefficient metabolism in support of denitratation due to a less direct assimilability of glycerol, or the downstream delivery of electrons on the electron transport chain similar to methanol.[16,17]

Likely contributing factors to the need for a higher than the theoretical influent COD:$NO_3^-$-N ratio (see SI) were COD uptake for cell maintenance and synthesis[34] and intracellular storage,[39] or an incomplete enrichment for a solely denitratating or progressive onset[40] phenotype-dominated microbial community. The presence of non-denitrifying heterotrophic microorganisms,[35] or those heterotrophs that express either a complete denitrification metabolic pathway or a rapid, complete onset of denitrification genes[40] would impose a competitive demand on influent COD. Competition for influent COD by microorganisms exhibiting these phenotypes would decrease its availability for selective reduction of $NO_3^-$ to $NO_2^-$ thus requiring influent COD:$NO_3^-$-N ratios above that determined theoretically, which was supported by the results herein (Table 1).

### 3.2. Process Kinetics

Notably, extant kinetic analysis indicated that transient $NO_2^-$ accumulation at all influent COD:$NO_3^-$-N ratios assessed was potentially due to at least one order of magnitude greater specific rates of $NO_3^-$ reduction compared to the specific rates of $NO_2^-$ reduction driven by glycerol (Table 2).[41] Observed performance at influent COD:$NO_3^-$-N>3.0:1 (Fig. S2) also

supported this assertion as the maximum $NO_2^-$ accumulated never equaled the initial $NO_3^-$ concentration, indicating that there was concomitant reduction of $NO_3^-$ and $NO_2^-$. However, performance at influent COD:$NO_3^-$-N=3.0:1 resulted in near-complete selective reduction of $NO_3^-$ to $NO_2^-$ prior to terminal reduction to $N_2$ gas (Fig. S2). It should be emphasized that the kinetic profiles in Fig. S2 were obtained from acclimated biomass from individual SBRs operated for at least 4 x SRT at each influent COD:$NO_3^-$-N ratio.

In general, measured specific rates of $NO_3^-$ reduction and $\mu_{max}$ values were higher than those previously reported for glycerol-driven full denitrification studies (Table 2) and may be due to differences in the microbial community that was selected for by stoichiometric limitation during our current denitratation-specific study. Glycerol-driven specific rates of $NO_3^-$ reduction values were nearly double those reported for acetate-driven systems at similar influent COD:$NO_3^-$-N ratios, but slightly lower than those observed in an experiment utilizing a combination of external COD sources garnered from sodium acetate and endogenous carbon in a domestic wastewater stream (Table 2). The ratios of sDNaR:sDNiR achieved in this study with glycerol across different influent COD:$NO_3^-$-N values were also higher than previously reported with acetate (Table 2). This difference may be due to variations in the direct assimilability of each COD source with more assimilable COD sources such as glycerol or endogenous carbon in these cases supporting greater specific rates of $NO_3^-$ reduction,[34] or the COD source-supported microbial community.

### 3.3. $NO_2^-$ Accumulation through the Management of Operational Controls

#### 3.3.1. Denitratation Control via Batch Duration

Batch duration was identified as an effective process control parameter to maximize $NO_2^-$ accumulation. The duration of the anoxic feed and react period could be shortened to achieve comparable or improved performance. $NO_2^-$ concentrations decreased following peaks of $NO_2^-$ accumulation at higher influent COD:$NO_3^-$-N ratios (4.0:1, 5.0:1; Fig. 2). This decrease was not observed at influent COD:$NO_3^-$-N=3.0:1, indicating that excess COD remained following completion of denitratation at higher ratios. Despite minimal $NO_2^-$ reduction following peak $NO_2^-$ accumulation at influent COD:$NO_3^-$-N=2.5:1, overall performance remained low, making this ratio less effective at achieving partial denitratation (Table 1; Fig. 2).

Results generally supported that influent COD:$NO_3^-$-N ratios have an inverse relationship with time to maximum $NO_2^-$ accumulation during the anoxic react period. Batch duration could be reduced to 150 minutes or less, or the time to maximum $NO_2^-$ accumulation (Fig. 2). Subtraction of the feed and react period of the SBR cycle from the reduced batch duration, by extension, would yield an optimal react time equivalent to a continuous flow system's HRT (Fig. 2). The optimal react time is representative of when glycerol is available for $NO_3^-$ reduction in both systems. Therefore, the identified optimal react times in our SBR system would be equivalent to HRTs of approximately 30 minutes (COD:$NO_3^-$-N=4.0:1 and 5.0:1) to 60 minutes (COD:$NO_3^-$-N=2.5:1 and 3.0:1) in continuous flow systems operating at each respective influent COD:$NO_3^-$-N ratio.

403 3.3.2. Denitratation Control via pH and ORP

404 During unbuffered (see SI) and non-carbon limited operation (influent COD:$NO_3^-$-N≥5.9:1),
405 the denitratation-dominated phase of the denitrification profile exhibited a distinct decrease in the
406 reactor's pH and increase in the ORP until both reached inflection points after which pH increased
407 and ORP decreased (Fig. 3). At this inflection point, $NO_3^-$ reduction decelerated due to the
408 depletion of available $NO_3^-$ allowing for observable concomitant $NO_2^-$ reduction thus decreasing
409 the NAR and negatively impacting the objective of maximizing $NO_2^-$ accumulation. Continuous
410 monitoring of pH and ORP could provide an observable real-time control to maximize
411 denitratation. While feedforward online control of COD dosing tied to influent $NO_x$ loading has
412 proven effective in controlling denitratation,[19] this system requires online $NO_x$ sensors which
413 may not be achievable at all plants due to potentially high capital[42] and maintenance costs.[43]
414 Rather, denitratation control via pH and ORP observation could provide a backup check or serve
415 as a less costly alternative[42] with widely available and utilized sensors.

416 pH and ORP were previously reported as control parameters for denitrification driven by
417 acetate, methanol, endogenous carbon, soybean wastewater, and brewery wastewater.[7,8,36,44,45]
418 Contrary to the distinct glycerol-driven pH and ORP profile observed in the current study, Ge et
419 al.[8] and Du et al.[7] described acetate-driven profiles exhibiting a general increase in pH whereby a
420 "turning point" separated denitratation from denitritation. However, the observed pH profiles
421 obtained experimentally in our study (Fig. 3) are in excellent concurrence with theoretically
422 calculated net production of 0.43 equivalents of acidity per mole $NO_3^-$ reduced to $NO_2^-$ (Eqn. 5),
423 which supported the observed pH fluctuation profiles.

424

425 $$NO_3^- + (0.14)C_3H_8O_3 \rightleftarrows NO_2^- + (0.43)CO_2 + (0.57)H_2O$$ **Eqn. 5**

For completeness, stoichiometry (Eqn. 6) reveals that denitritation should result in a net consumption of 0.36 equivalents of acidity per mole $NO_2^-$ reduced to $N_2$ gas at pH 7.5.

$$NO_2^- + (0.21)C_3H_8O_3 + H^+ \rightleftarrows (0.50)N_2 + (0.64)CO_2 + (1.36)H_2O \quad \textbf{Eqn. 6}$$

3.3.3. Denitratation Control via Feeding Strategy

The pulse feeding strategy resulted in a statistically significant improvement in denitratation performance ($\alpha$=0.05; n=8) over the semi-continuous feeding strategy in both $NO_2^-$ accumulation (p=0.03) and $NO_3^-$ reduction (p=0.0003), indicating that feeding methodology impacted the performance of the system (Table S4). As both feeding strategies maintained equivalent influent COD:$NO_3^-$-N ratio per substrate pulse or for the duration of the semi-continuous feeding period, this difference in system performance was thought to be influenced by the temporal distribution of substrate pulses. Those pulses occurring later in the anoxic feed and react period may have limited the time for the biotransformation of $NO_3^-$ to gaseous nitrogen thus allowing for greater $NO_2^-$ accumulation. This is counter to the semi-continuous feeding strategy, where fully denitrifying microorganisms within the microbial community had the full anoxic feed and react period to reduce influent $NO_3^-$. Therefore, in a continuous-flow BNR process, the spatial location of introducing glycerol could be another factor to promote partial denitratation if possible. Optimizing the dosing location of electron donors is quite widely practiced for increasing the efficiency of COD utilization even for full denitrification in step-feed BNR or Bardenpho configurations.[12]

### 3.4. Microbial Ecology

*Proteobacteria* was the most dominant phylum out of 14 identified at all influent COD:$NO_3^-$-N ratios (Fig. 4a). *β-Proteobacteria* made up at least 73% of the *Proteobacteria* phylum at all influent COD:$NO_3^-$-N ratios. In a survey of wastewater denitrifying bacterial 16S rDNA sequences retrieved from GenBank, Lu et al.[46] found that approximately 72% of prokaryotic microorganisms displaying denitrifying capabilities were taxonomically affiliated with *Proteobacteria*, while *β* sub-class affiliated microorganisms were typically abundant in denitrifying activated sludge,[2,46,47] similar to the findings herein.

Within *β-Proteobacteria*, the *Rhodocyclaceae* and *Comamonadaceae* families were identified as those mainly involved in denitrification in activated sludge.[47,48] Our findings supported this as *Thauera* sp., belonging to the *Rhodocyclaceae* family within *β-Proteobacteria*, was enriched as the most dominant genus with a relative abundance of nearly 80% at influent COD:$NO_3^-$-N=3.0:1 (Fig. 4b). While widely found in denitrifying activated sludge systems,[46] *Comamonadaceae* fam. was not identified in this study, indicating that their enrichment may not be favored under stoichiometrically-limited conditions imposed herein. The microbial communities at influent COD:$NO_3^-$-N=3.0:1, 4.0:1, and 5.0:1 were similar, while that at influent COD:$NO_3^-$-N=2.5:1 was dissimilar from all others according to Principal Coordinates Analysis (PCoA; Fig. S3) at the species taxonomic level. Both Chao-1 estimations[49] and Shannon's diversity indices[50] further indicated that species richness decreased as influent COD:$NO_3^-$-N approached influent COD:$NO_3^-$-N=3.0:1 with the richness at influent COD:$NO_3^-$-N=2.5:1 being much greater than the other ratios examined (Table S5). The distinct difference in the microbial community structure at influent COD:$NO_3^-$-N=2.5:1 compared to other influent COD:$NO_3^-$-N

ratios examined (Fig. 4b; Fig. S3; Table S5) indicated that the influent COD:$NO_3^-$-N ratio was an important factor in the selection and regulation of the microbial community structure.[51,52]

Influent COD:$NO_3^-$-N=3.0:1 presented the greatest relative abundance of *Thauera* sp. (80%) which subsequently decreased (66% and 61% at influent COD:$NO_3^-$-N=4.0:1 and 5.0:1, respectively) as influent COD:$NO_3^-$-N increased. *Burkholderiaceae* fam. and *Paracoccus* sp. persisted at elevated enrichment levels across the range of stoichiometrically-limited influent COD:$NO_3^-$-N ratios examined (Fig. 4b). Other studies identified both taxa as widely present in heterotrophic denitrification systems[53–55] with certain members able to express complete denitrification pathways using myriad carbon sources.[54,56,57] Their combined increase in relative abundance as influent COD:$NO_3^-$-N approached the theoretical requirement for complete denitrification (5.9:1; see SI) coincided with increased fully-denitrifying performance (Fig. 1). The decrease in the competitive demand for stoichiometrically-limited influent COD likely led to a greater enrichment of microorganisms capable of expressing a complete denitrification metabolic pathway or a rapid, complete onset of denitrification genes.[40] *Saccharimondaceae* fam., of Candidate phylum *Saccharibacteria*, persisted at all influent COD:$NO_3^-$-N ratios examined and has been reported to prefer complex organic substrates typically resulting from endogenously-released compounds in activated sludge systems.[58,59]

The structural change at influent COD:$NO_3^-$-N=2.5:1 corresponded with the decrease in influent COD:$NO_3^-$-N below the identified optimal ratio (3.0:1) and a deterioration in reactor performance (Fig. 1). While NAR was not significantly different, a low NRR (54%; Table 1) at influent COD:$NO_3^-$-N=2.5:1 indicated that the selective pressure of insufficient influent COD may have selected for microorganisms more capable of growth in the substrate-limited conditions.[12] Those taxa previously mentioned remained similarly enriched; however, *Thauera*

494 sp. relative abundance decreased to 24%, indicating non-optimal conditions were present to
495 support glycerol-driven denitratation. *Rhizobiaceae* fam., reportedly able to express a complete
496 metabolic denitrification pathway,[60] and *Prosthecobacter* sp., an oligotroph that thrives in
497 nutrient-poor conditions,[61] were enriched at influent COD:$NO_3^-$-N=2.5:1 (4% and 6% relative
498 abundance, respectively). Both taxa presented negligible reads at all other influent COD:$NO_3^-$-N
499 ratios examined suggesting that they may have been able to outcompete *Thauera* sp. for the
500 limited influent COD at influent COD:$NO_3^-$-N=2.5:1.

501 Certain *Thauera* spp. strains have been characterized according to two distinct regulatory
502 phenotypes,[62] including the immediate and simultaneous onset of all denitrification genes with
503 no detectable $NO_2^-$ accumulation, as well as the progressive and sequential onset of
504 denitrification cascade genes with appreciable $NO_2^-$ accumulation.[40] Selective pressures were
505 not identified for either in the current study, although the selection for progressive onset
506 denitrifiers would be critical to facilitate denitratation. The coupling of a high relative
507 abundance of *Thauera* sp. (Fig. 4b), high NRR, and high NAR (Table 1), with the ability to
508 perform full denitrification when presented with sufficient COD (Fig. S2) indicated that the
509 application of stoichiometric limitation in the influent COD:$NO_3^-$-N as a selective pressure may
510 favor the progressive onset over rapid, complete onset phenotype. *Thauera* sp. may represent a
511 key functional microorganism for denitratation systems indicated by its decreasing relative
512 abundances away from the optimal influent COD:$NO_3^-$-N (Fig. 4b). Several recent denitratation-
513 specific studies[5,7,10,63] further supported this argument with reported *Thauera* sp. relative
514 abundances from 55% to 73% under limited influent COD:$NO_3^-$-N ratios with acetate as the
515 external COD source despite different seed sludges. In comparison, acetate-driven full
516 denitrification studies reported no more than 12% relative abundance of *Thauera* sp.[47,64]

Therefore, the application of a stoichiometrically-limited influent COD:$NO_3^-$-N ratio as a selective pressure in a denitratation system may impart a stronger impact on the denitrifying community structure than previously recognized.

## 4. Conclusions

Denitratation, with downstream anammox processes, offers chemical and energy reductions through resource-efficient BNR of $NH_4^+$ and $NO_3^-$-laden waste streams. A fundamentally-based, first-principles approach was used to propose an influent COD:N ratio and other operating parameters that would promote denitratation and experimental results aligned with expectations. Glycerol supported the process kinetics and microbial ecology necessary to selectively convert $NO_3^-$ to $NO_2^-$ in denitratation systems. Process control strategies, including influent COD loading and pH, ORP, and batch duration operational setpoints were identified and used to further define reactor operating strategies that could maximize denitratation performance. Significant enrichment indicated *Thauera* sp. may represent a key functional microorganism in denitratation systems. This study implicated stoichiometric limitation of influent organic carbon, unique microbial community enrichment, and differential $NO_3^-$ and $NO_2^-$ reduction kinetics as determinant factors in glycerol-driven denitratation.

## ADDITIONAL INFORMATION

E-supplementary data can be found in online version of the paper.

## AUTHOR INFORMATION

**ORCID**

Matthew Baideme: 0000-0002-2556-0624

Kartik Chandran: 0000-0002-7526-3724

**Author Contributions:** The manuscript was written through contributions of all authors. All authors gave approval to the final version of the manuscript. All authors contributed equally.

**Notes**: The authors declare no competing financial interests.

## ACKNOWLEDGMENTS

This study was supported by Project Director, Joint Services, project USMA1740. Views and opinions expressed or implied herein are solely those of the authors and should not be construed as policy or carrying the official sanction of the Department of Defense, United States Army, United States Military Academy, or other agencies or departments of the U.S. Government.

## REFERENCES

1 Y. Peng and G. Zhu, Biological nitrogen removal with nitrification and denitrification via nitrite pathway, *Appl. Microbiol. Biotechnol.*, 2006, **73**, 15–26.

2 C. S. Srinandan, M. Shah, B. Patel and A. S. Nerurkar, Assessment of denitrifying bacterial composition in activated sludge, *Bioresour. Technol.*, 2011, **102**, 9481–9489.

3 P. Cyplik, R. Marecik, A. Piotrowska-Cyplik, A. Olejnik, A. Drożdżyńska and Ł. Chrzanowski, Biological denitrification of high nitrate processing wastewaters from explosives production plant, *Water, Air, Soil Pollut.*, 2012, **223**, 1791–1800.

4 J. Shen, R. He, W. Han, X. Sun, J. Li and L. Wang, Biological denitrification of high-nitrate wastewater in a modified anoxic/oxic-membrane bioreactor (A/O-MBR), *J. Hazard. Mater.*, 2009, **172**, 595–600.

5 S. Cao, R. Du, B. Li, S. Wang, N. Ren and Y. Peng, Nitrite production from partial-denitrification process fed with low carbon/nitrogen (C/N) domestic wastewater: performance, kinetics and microbial community, *Chem. Eng. J.*, 2017, **326**, 1186–1196.

6 S. Cao, S. Wang, Y. Peng, C. Wu, R. Du, L. Gong and B. Ma, Achieving partial denitrification with sludge fermentation liquid as carbon source: The effect of seeding sludge, *Bioresour. Technol.*, 2013, **149**, 570–574.

7 R. Du, Y. Peng, S. Cao, B. Li, S. Wang and M. Niu, Mechanisms and microbial structure of partial denitrification with high nitrite accumulation, *Appl. Microbiol. Biotechnol.*, 2016, **100**, 2011–2021.

8 S. Ge, Y. Peng, S. Wang, C. Lu, X. Cao and Y. Zhu, Nitrite accumulation under constant temperature in anoxic denitrification process: the effects of carbon sources and COD/$NO_3$-N, *Bioresour. Technol.*, 2012, **114**, 137–143.

9 W. Li, X.-Y. Lin, J.-J. Chen, C.-Y. Cai, G. Abbas, Z.-Q. Hu, H.-P. Zhao and P. Zheng, Enrichment of denitratating bacteria from a methylotrophic denitrifying culture, *Appl. Microbiol. Biotechnol.*, 2016, **100**, 10203–10213.

10 Z. Si, Y. Peng, A. Yang, S. Zhang, B. Li, B. Wang and S. Wang, Rapid nitrite production via partial denitrification: pilot-scale operation and microbial community analysis, *Environ. Sci.: Water Res. Technol.*, 2018, **4**, 80–86.

11 L. Russ, D. R. Speth, M. S. M. Jetten, H. J. M. Op den Camp and B. Kartal, Interactions between anaerobic ammonium and sulfur-oxidizing bacteria in a laboratory scale model system: Anaerobic ammonium and sulfur-oxidizing coculture, *Environ. Microbiol.*, 2014, **16**, 3487–3498.

12 C. P. L. Grady, G. T. Daigger, N. G. Love and C. D. M. Filipe, *Biological Wastewater Treatment*, CRC Press, Boca Raton, FL, 3rd edn., 2011.

13 K. Hanaki, Z. Hong and T. Matsuo, Production of nitrous oxide gas during denitrification of wastewater, *Water Sci. Technol.*, 1992, **26**, 1027–1036.

14 V. Baytshtok, H. Lu, H. Park, S. Kim, R. Yu and K. Chandran, Impact of varying electron donors on the molecular microbial ecology and biokinetics of methylotrophic denitrifying bacteria, *Biotechnol. Bioeng.*, 2009, **102**, 1527–1536.

15 D. Richardson, H. Felgate, N. Watmough, A. Thomson and E. Baggs, Mitigating release of the potent greenhouse gas $N_2O$ from the nitrogen cycle – could enzymic regulation hold the key?, *Trends in Biotechnology*, 2009, **27**, 388–397.

16 J. van Rijn, Y. Tal and Y. Barak, Influence of volatile fatty acids on nitrite accumulation by a *Pseudomonas stutzeri* strain isolated from a denitrifying fluidized bed reactor, *Appl. Environ. Microbiol.*, 1996, **62**, 2615–2620.

17 H. W. van Verseveld and A. H. Stouthamer, Electron-transport chain and coupled oxidative phosphorylation in methanol-grown *Paracoccus denitrificans*, *Arch. Microbiol.*, 1978, **118**, 13–20.

18 J. Hinojosa, R. Riffat, S. Fink, S. Murthy, K. Selock, C. Bott, I. Takacs, P. Dold and R. Wimmer, in *Proceedings of the 81st Annual Water Environment Federation Technical Exposition and Conference*, Chicago, 2008, pp. 274–288.

19 T. Le, B. Peng, C. Su, A. Massoudieh, A. Torrents, A. Al-Omari, S. Murthy, B. Wett, K. Chandran, C. deBarbadillo, C. Bott and H. De Clippeleir, Nitrate residual as a key parameter to efficiently control partial denitrification coupling with anammox, *Water Environ. Res.*, 2019, **91**, 1455–1465.

20 Y. Mokhayeri, R. Riffat, S. Murthy, W. Bailey, I. Takacs and C. Bott, Balancing yield, kinetics and cost for three external carbon sources used for suspended growth post-denitrification, *Water Science & Technology*, 2009, **60**, 2485.

21 G. P. da Silva, M. Mack and J. Contiero, Glycerol: A promising and abundant carbon source for industrial microbiology, *Biotechnol. Adv.*, 2009, **27**, 30–39.

22 H. Lu and K. Chandran, Diagnosis and quantification of glycerol assimilating denitrifying bacteria in an integrated fixed-film activated sludge reactor via $^{13}C$ DNA stable-isotope probing, *Environ. Sci. Technol.*, 2010, **44**, 8943–8949.

23 D. Güven, A. Dapena, B. Kartal, M. C. Schmid, B. Maas, K. van de Pas-Schoonen, S. Sozen, R. Mendez, H. J. M. Op den Camp, M. S. M. Jetten, M. Strous and I. Schmidt, Propionate oxidation by and methanol inhibition of anaerobic ammonium-oxidizing bacteria, *Appl. Environ. Microbiol.*, 2005, **71**, 1066–1071.

24 H. Park, A. C. Brotto, M. C. M. van Loosdrecht and K. Chandran, Discovery and metagenomic analysis of an anammox bacterial enrichment related to *Candidatus* "Brocadia caroliniensis" in a full-scale glycerol-fed nitritation-denitritation separate centrate treatment process, *Water Res.*, 2017, **111**, 265–273.

25 American Public Health Association, *Standard Methods for the Examination of Water and Wastewater*, American Public Health Association, American Water Works Association, Water Environment Federation, Washington, DC, 23rd edn., 2017.

26 E. M. Contreras, N. C. Bertola, L. Giannuzzi and N. E. Zaritzky, A modified method to determine biomass concentration as COD in pure cultures and in activated sludge systems, *Water SA*, 2002, **28**, 463–468.

27 P. D. Schloss, S. L. Westcott, T. Ryabin, J. R. Hall, M. Hartmann, E. B. Hollister, R. A. Lesniewski, B. B. Oakley, D. H. Parks, C. J. Robinson, J. W. Sahl, B. Stres, G. G. Thallinger, D. J. V. Horn and C. F. Weber, Introducing mothur: Open-source, platform-independent, community-supported software for describing and comparing microbial communities, *Appl. Environ. Microbiol.*, 2009, **75**, 7537–7541.

28 S. Chen, T. Huang, Y. Zhou, Y. Han, M. Xu and J. Gu, AfterQC: automatic filtering, trimming, error removing and quality control for fastq data, *BMC Bioinf.*, 2017, **18**, 91–100.

29 B. J. Callahan, P. J. McMurdie, M. J. Rosen, A. W. Han, A. J. A. Johnson and S. P. Holmes, DADA2: High-resolution sample inference from Illumina amplicon data, *Nat. Methods*, 2016, **13**, 581–583.

30 J. G. Caporaso, J. Kuczynski, J. Stombaugh, K. Bittinger, F. D. Bushman, E. K. Costello, N. Fierer, A. G. Pena, J. K. Goodrich and J. I. Gordon, QIIME allows analysis of high-throughput community sequencing data, *Nat. Methods*, 2010, **7**, 335–336.

31 R. Du, Y. Peng, S. Cao, S. Wang and C. Wu, Advanced nitrogen removal from wastewater by combining anammox with partial denitrification, *Bioresour. Technol.*, 2015, **179**, 497–504.

32 P. L. McCarty, Thermodynamic electron equivalents model for bacterial yield prediction: Modifications and comparative evaluations, *Biotechnol. Bioeng.*, 2007, **97**, 377–388.

33 N. Chamchoi, S. Nitisoravut and J. E. Schmidt, Inactivation of ANAMMOX communities under concurrent operation of anaerobic ammonium oxidation (ANAMMOX) and denitrification, *Bioresour. Technol.*, 2008, **99**, 3331–3336.

34 H. Constantin and M. Fick, Influence of C-sources on the denitrification rate of a high-nitrate concentrated industrial wastewater, *Water Res.*, 1997, **31**, 583–589.

35 G. D. Drysdale, H. C. Kasan and F. Bux, Assessment of denitrification by the ordinary heterotrophic organisms in an NDBEPR activated sludge system, *Water Sci. Technol.*, 2001, **43**, 147–154.

36 H. Sun, Q. Yang, Y. Peng, X. Shi, S. Wang and S. Zhang, Nitrite accumulation during the denitrification process in SBR for the treatment of pre-treated landfill leachate, *Chin. J. Chem. Eng.*, 2009, **17**, 1027–1031.

37 R. Du, S. Cao, M. Niu, B. Li, S. Wang and Y. Peng, Performance of partial-denitrification process providing nitrite for anammox in sequencing batch reactor (SBR) and upflow sludge blanket (USB) reactor, *Int. Biodeterior. Biodegrad.*, 2017, **122**, 38–46.

38 D. Güven, Effects of different carbon sources on denitrification efficiency associated with culture adaptation and C/N ratio, *Clean: Soil, Air, Water*, 2009, **37**, 565–573.

39 M. C. M. van Loosdrecht, M. A. Pot and J. J. Heijnen, Importance of bacterial storage polymers in bioprocesses, *Water Sci. Technol.*, 1997, **35**, 41–47.

40 B. Liu, Y. Mao, L. Bergaust, L. R. Bakken and Å. Frostegård, Strains in the genus *Thauera* exhibit remarkably different denitrification regulatory phenotypes, *Environ. Microbiol.*, 2013, **15**, 2816–2828.

41 M. R. Betlach and J. M. Tiedje, Kinetic explanation for accumulation of nitrite, nitric oxide, and nitrous oxide during bacterial denitrification, *Appl. Environ. Microbiol.*, 1981, **42**, 1074–1084.

42 J. Dries, Dynamic control of nutrient-removal from industrial wastewater in a sequencing batch reactor (SBR), using common and low-cost online sensors, *Water Sci. Technol.*, 2015, **73**, 740–745.

43 L. Åmand, G. Olsson and B. Carlsson, Aeration control – a review, *Water Sci. Technol.*, 2013, **67**, 2374–2398.

44 L. Gong, M. Huo, Q. Yang, J. Li, B. Ma, R. Zhu, S. Wang and Y. Peng, Performance of heterotrophic partial denitrification under feast-famine condition of electron donor: A case study using acetate as external carbon source, *Bioresour. Technol.*, 2013, **133**, 263–269.

45 Y. Z. Peng, J. F. Gao, S. Y. Wang and M. H. Sui, Use pH and ORP as fuzzy control parameters of denitrification in SBR process, *Water Sci. Technol.*, 2002, **46**, 131–137.

46 H. Lu, K. Chandran and D. Stensel, Microbial ecology of denitrification in biological wastewater treatment, *Water Res.*, 2014, **64**, 237–254.

47 M. P. Ginige, J. Keller and L. L. Blackall, Investigation of an acetate-fed denitrifying microbial community by stable isotope probing, full-cycle rRNA analysis, and fluorescent in situ hybridization-microautoradiography, *Appl. Environ. Microbiol.*, 2005, **71**, 8683–8691.

48 C. Etchebehere, I. Errazquin, E. Barrandeguy, P. Dabert and R. Moletta, Evaluation of the denitrifying microbiota of anoxic reactors, *FEMS Microbiol. Ecol.*, 2001, **35**, 259–265.

49 A. Chao, C. Chiu, T. C. Hsieh, T. Davis, D. A. Nipperess and D. P. Faith, Rarefaction and extrapolation of phylogenetic diversity, *Methods Ecol. Evol.*, 2015, **6**, 380–388.

50 A. E. Magurran, *Measuring Biological Diversity*, Blackwell Science Ltd., Malden, MA, 1st edn., 2004.

51 E. Szabó, R. Liébana, M. Hermansson, O. Modin, F. Persson and B.-M. Wilén, Microbial population dynamics and ecosystem functions of anoxic/aerobic granular sludge in sequencing batch reactors operated at different organic loading rates, *Front. Microbiol.*, , DOI:10.3389/fmicb.2017.00770.

52 C. Chen, M. Zhang, X. Yu, J. Mei, Y. Jiang, Y. Wang and T. C. Zhang, Effect of C/N ratios on nitrogen removal and microbial communities in the anaerobic baffled reactor (ABR) with an anammox-coupling-denitrification process, *Water Sci. Technol.*, 2018, **78**, 2338–2348.

53 X.-Y. Fan, J.-F. Gao, K.-L. Pan, D.-C. Li and H.-H. Dai, Temporal dynamics of bacterial communities and predicted nitrogen metabolism genes in a full-scale wastewater treatment plant, *RSC Adv.*, 2017, **7**, 56317–56327.

54 S. A. Hetz and M. A. Horn, *Burkholderiaceae* are key acetate assimilators during complete denitrification in acidic cryoturbated peat circles of the Arctic Tundra, *Front. Microbiol.*, 2021, **12**, 628269.

55 K. C. Wrighton, B. Virdis, P. Clauwaert, S. T. Read, R. A. Daly, N. Boon, Y. Piceno, G. L. Andersen, J. D. Coates and K. Rabaey, Bacterial community structure corresponds to performance during cathodic nitrate reduction, *ISME J.*, 2010, **4**, 1443–1455.

56 E. F. DeLong, E. Stackebrandt, S. Lory and F. Thompson, Eds., *The Prokaryotes*, Springer, Berlin, Heidelberg, 4th edn.

57 M. Blaszczyk, Effect of medium composition on the denitrification of nitrate by *Paracoccus denitrificans*, *Appl. Environ. Microbiol.*, 1993, **59**, 3951–3953.

58 T. Kindaichi, S. Yamaoka, R. Uehara, N. Ozaki, A. Ohashi, M. Albertsen, P. H. Nielsen and J. L. Nielsen, Phylogenetic diversity and ecophysiology of Candidate phylum Saccharibacteria in activated sludge, *FEMS Microbiol. Ecol.*, 2016, **92**, fiw078.

59 J. Zhao, Y. Li, X. Chen and Y. Li, Effects of carbon sources on sludge performance and microbial community for 4-chlorophenol wastewater treatment in sequencing batch reactors, *Bioresour. Technol.*, 2018, **255**, 22–28.

719 60 J. J. Rich, R. S. Heichen, P. J. Bottomley, K. Cromack and D. D. Myrold, Community
720 composition and functioning of denitrifying bacteria from adjacent meadow and forest soils,
721 *Appl. Environ. Microbiol.*, 2003, **69**, 5974–5982.
722 61 X. Wang, M. Hu, Y. Xia, X. Wen and K. Ding, Pyrosequencing analysis of bacterial
723 diversity in 14 wastewater treatment systems in China, *Appl. Environ. Microbiol.*, 2012, **78**,
724 7042–7047.
725 62 L. Bergaust, L. R. Bakken and Å. Frostegård, Denitrification regulatory phenotype, a new
726 term for the characterization of denitrifying bacteria, *Biochem. Soc. Trans.*, 2011, **39**, 207–
727 212.
728 63 R. Du, S. Cao, B. Li, M. Niu, S. Wang and Y. Peng, Performance and microbial community
729 analysis of a novel DEAMOX based on partial-denitrification and anammox treating
730 ammonia and nitrate wastewaters, *Water Res.*, 2017, **108**, 46–56.
731 64 T. R. Thomsen, Y. Kong and P. H. Nielsen, Ecophysiology of abundant denitrifying bacteria
732 in activated sludge, *FEMS Microbiol. Ecol.*, 2007, **60**, 370–382.
733 65 C. Glass and J. Silverstein, Denitrification kinetics of high nitrate concentration water: pH
734 effect on inhibition and nitrite accumulation, *Water Res.*, 1998, **32**, 831–839.
735

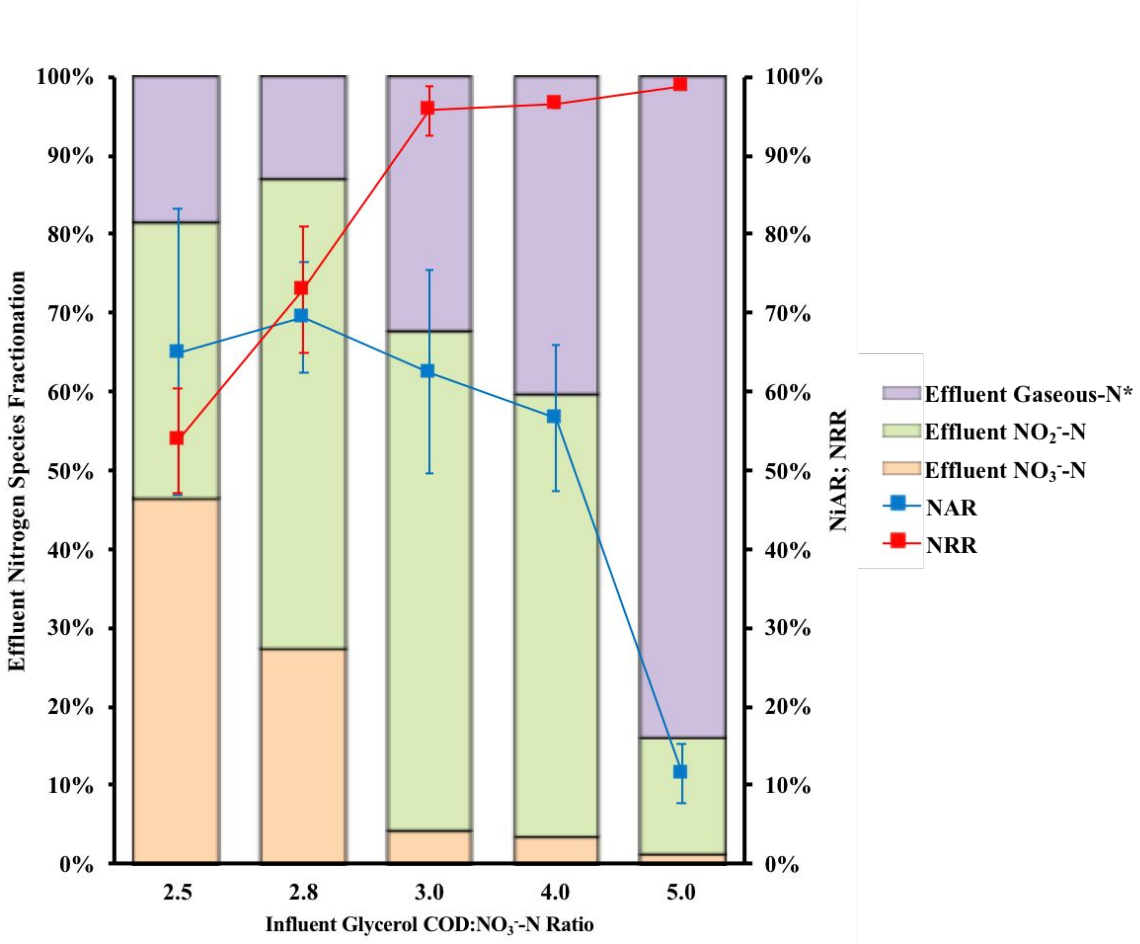


736

737 ***Figure 1.*** *Steady-state denitratation performance and respective NAR and NRR assessed at each*

738 *influent COD:$NO_3^-$-N ratio. *Effluent gaseous-N contributions were calculated via mass balance.*

739

740 ***Table 1.*** *Influence of external COD source and influent COD:$NO_3^-$-N ratios on denitratation*

741 *performance.*

| External COD Source | Influent COD:$NO_3^-$-N | NAR [%] | NRR [%] | Reactor Type | Source |
|---|---|---|---|---|---|
| Sodium Acetate | 3.0 | 51–73 | ~73–93 | USB[a] | 37 |
| | 3.0 | 80 | ~100 | SBR | 7 |
| | 2.75 | 83 | ~100 | | 37 |
| | 2.5 | 87 | 85 | | 10 |
| Sodium Acetate / Domestic Wastewater | 3.1[b] | 90 | ~100 | | 5 |
| Fermentation Effluent | 3.0 | 80 | ~100 | | 6 |
| Glycerol | 2.5 | 65±18 | 54±7 | | This study |
| | 2.8 | 69±7 | 73±8 | | |
| | 3.0 | 62±13 | 96±3 | | |
| | 4.0 | 57±9 | 97±1 | | |
| | 5.0 | 11±4 | 99±0 | | |

[a] Upflow sludge blanket reactor (USB)
[b] Reported influent ratio includes COD associated both with the domestic wastewater and external COD source

742

743

744 ***Table 2.*** *Summary of process kinetic parameters for both full denitrification and denitratation*

745 *studies with respect to external COD source and influent COD:$NO_3^-$-N ratio.*

| COD Source | Inf. COD:$NO_3^-$-N | Inf. $NO_3^-$-N [mg N/L] | $\mu_{max}$ [$d^{-1}$] | sDNaR[h] [mg N/g VSS/h] | sDNiR[i] [mg N/g VSS/h] | Source |
|---|---|---|---|---|---|---|
| Sodium Acetate | 1.22 | 2,700 | -- | 23.0[f] | 19.0[f] | 65 |
| | 5.0 | 150 | -- | 82.3 | 32.0 | 7 |
| | 1.0 | -- | -- | 52.0 | -- | 8 |
| | 6.0 | -- | -- | 280.0 | -- | |
| Sodium Acetate / Domestic WW | 3.4[e] | 1,000 | -- | 190.0 | -- | 5 |
| Glycerol | 5.0 | 100 | -- | 6.5[a,d] | | 22 |
| | 26.0 | 22.5 | 3.4 | 1.7[a,b] | | 18 |
| | 26.0 | 22.5 | 2.0 | 1.35[a,c] | | |
| | 2.5 | 100 | -- | 112.3 | 1.8 | This Study |
| | 3.0 | 100 | -- | 135.3 | 14.9 | |
| | 5.0 | 100 | -- | 147.1 | 40.0 | |
| | 20.0[g] (Unlimited) | 100 | 6.2 | -- | -- | |

[a] Rates reported as mg $NO_x$-N/g VSS/hr based upon full denitrification studies.
[b] Rate reported in study exhibiting no $NO_2^-$ accumulation.
[c] Rate reported in study exhibiting $NO_2^-$ accumulation.
[d] Suspended phase rates reported; biofilm rates not reported for comparison purposes to current study.
[e] Reported influent ratio includes COD associated both with the domestic wastewater and external COD source.
[f] Rates reported from original study for the pH utilized in current study.
[g] Batch experiment used biomass acclimated to influent COD:$NO_3^-$-N=3.0.
[h] Specific rate of $NO_3^-$ reduction (sDNaR)
[I] Specific rates of $NO_2^-$ reduction (sDNiR)

746

747

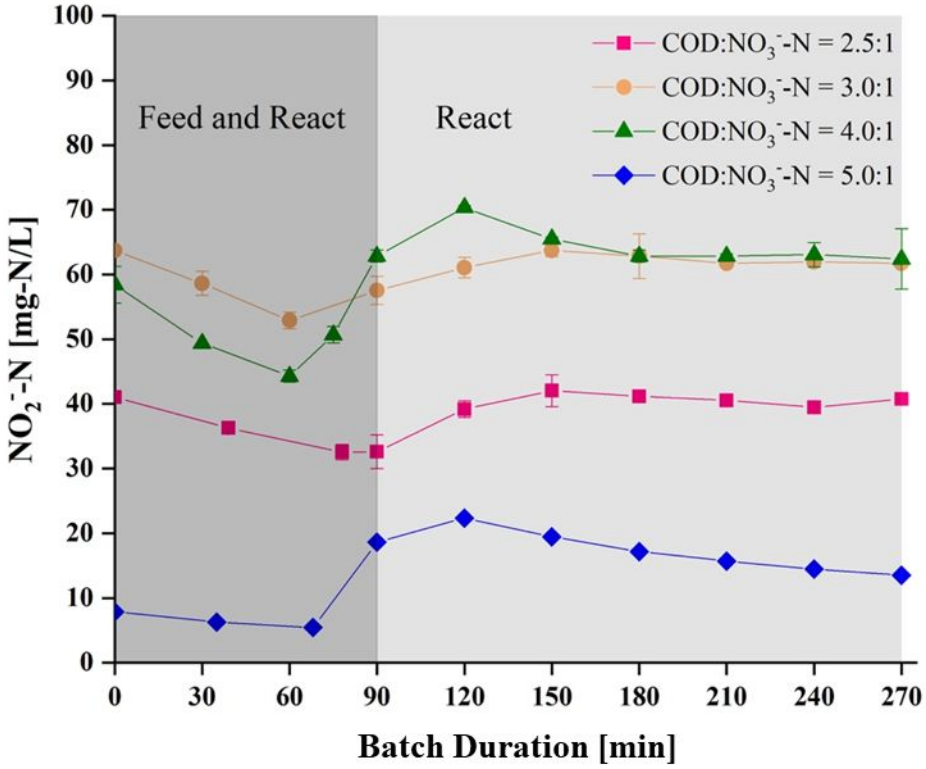


748

749 ***Figure 2.*** *Representative in situ $NO_2^-$-N profiles identified the optimal batch duration obtained*

750 *during steady-state operation at each respective influent COD:$NO_3^-$-N ratio. Optimal batch*

751 *durations corresponded to the points of maximum $NO_2^-$ accumulation at each respective influent*

752 *COD:$NO_3^-$-N ratio. Decreases in $NO_2^-$ concentrations during the feed and react period were*

753 *attributed to dilution.*

754

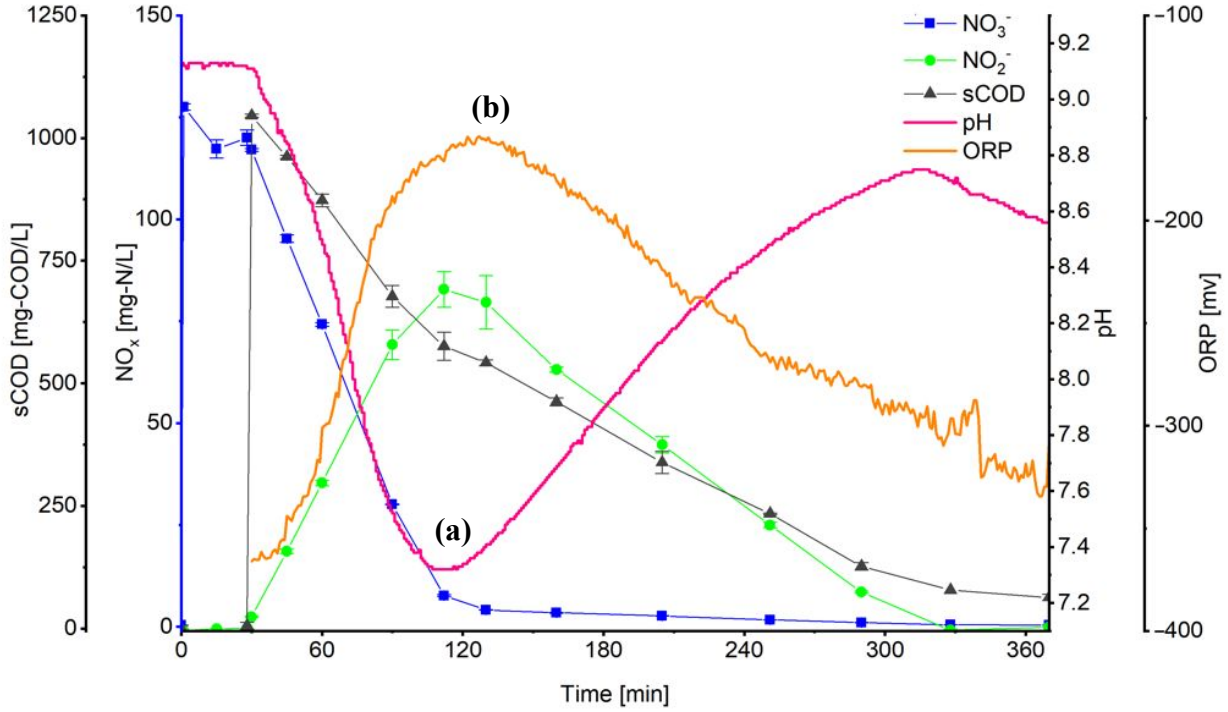


**Figure 3.** *$NO_x$, pH, and ORP profiles depicting the pH (a) and ORP (b) inflection points at the point of maximum $NO_2^-$ accumulation prior to which denitratation was dominant and after which denitritation became dominant (influent COD:$NO_3^-$-N=10.0:1; microbial ecology acclimated to influent COD:$NO_3^-$-N=3.0:1). Influent COD was provided in excess and beyond that at which biomass was acclimated in order to drive the process beyond denitratation and demonstrate the ability of pH and ORP to serve as denitratation process controls even under non-ideal influent COD:$NO_3^-$-N ratios.*

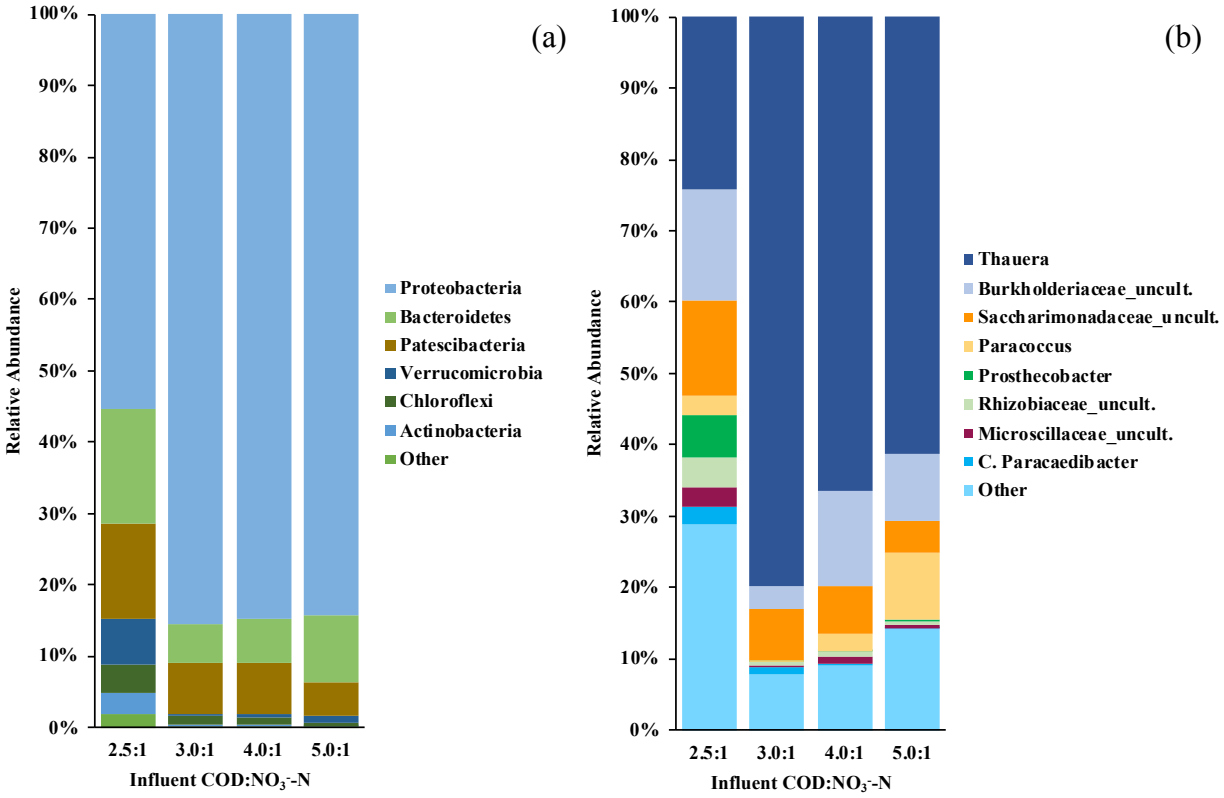


764

765 ***Figure 4.*** *Taxonomic analysis of the microbial consortium at the phylum (a) and genus (b)*

766 *taxonomic levels under optimal operating conditions (influent COD:$NO_3^-$-N=3.0:1, SRT=3 d).*

767 *The grouping "Other" comprises OTUs with less than 1% total relative abundance (among all*

768 *samples summed).*

769